# Multi-Domain Simulation of Transient Junction Temperatures and Resulting Stress-Strain Behavior of Power Switches for Long-Term Mission Profiles

Uwe Drofenik, Ivana Kovacevic, Roland Schmidt(*), Johann W. Kolar

ETH Zurich, PES / ETH Zentrum ETL H13, CH-8092 Zurich, Switzerland
Tel. +41-44 632 4267, Fax. +41-44-632 1212, drofenik@lem.ee.ethz.ch

(*) ABB Switzerland Ltd., Corporate Research, Segelhofstrasse 1K, CH-5405 Baden-Dättwil, Switzerland

***Abstract* - For lifetime estimation of power converters in traction applications, one method is to calculate numerically the stress-strain hysteresis curves of the interfaces silicon-solder-DCB and/or DCB-solder-baseplate inside the power modules. This can only be achieved if the transient junction temperatures in these layers are known for a defined mission-profile. Therefore, one has to couple circuit simulation with thermal simulation and stress-strain computation. The second challenge of this problem is to perform this transient simulation taking into account switching losses in the µs-range for mission profiles over a couple of minutes. In this paper we employ a new multi-domain simulation software to achieve results with reasonable computational effort.**

## I. Introduction

Switching frequencies typically define the smallest time-constants in a simulation. The numerical time steps have to be set at least by a factor 100 smaller then these time-constants. If the simulation has to be performed over long time periods, the number of time-steps and the according computational effort becomes huge. In lifetime estimation, mission profiles [1] lasting over a couple of minutes (e.g. 30 minutes for the European Driving Cycle) or even hours result in extremely time-consuming simulations, especially if the switching frequencies are high.

For lifetime estimation it is necessary to know the transient temperature distribution inside the power modules during the mission because temperature amplitude plus absolute temperature impact the lifetime of the power module [2], [3]. Calculating temperature distributions of three-dimensional structures is done with 3D-FEM software which comes with a very high computational effort (high memory consumption, very long simulation times). In case of coupled transient simulations it will be necessary to perform a 3D-thermal simulation at least every few time-steps of the circuit simulator which will result in unacceptably long simulation times. One solution is to extract a compact thermal model from the 3D-structure to describe the thermal behavior of the power module (including heat sink and cooling) employing a 3D-FEM simulator, and then employ this thermal compact model in a transient simulation of the circuit simulator. This will speed up the coupled simulation by orders of magnitude.

If physical models are employed in lifetime estimation, one has to set up a model of the stress-strain behavior of the material interfaces inside the power module where damage might occur. Such physical models describe effects like deformation and creep via differential equations. Input to the model is the transient temperature at the critical interface of the power module, and output of the physical model is the stress in dependency of the strain which typically results in a hysteresis curve where the area of the hysteresis loop is in approximation proportional to the deformation energy per load cycle. The physical model has to be parameterized based on preliminary cycling tests and/or material and geometry information from databases. Here, a large initial computational effort is necessary to parameterize the physical model correctly before feeding the simulated transient temperature data. Alternatively, performing the lifetime simulation after the transient temperatures have been simulated, the stress-strain computation could be performed directly coupled to the transient temperature simulation taking into account the effect of rising thermal resistances due to solder layer cracking and/or increasing losses at the wire-bond interfaces due to wire-bond lift-off.

The effort of such a complex coupled numerical simulation *circuit - thermal - reliability* is very high. In the following we show how to speed up the whole process employing multi-domain simulation software that has been developed at the PES / ETH Zurich especially for this type problem [4]. We will apply the procedure to the analysis of the power electronics of a wearable power supply [5].

## II. Example: Wearable Power Supply

The US Department of Defense organized a competition in 2008 with the goal defined as: "… Demonstrate a wearable electric power system providing 96 hours of equipment operation. The power system should attach to a vest and provide 20W average electric power for 96 hours with peak power requirements of up to 200W for short periods. All components, including the generation, storage,

electronics, and connections must weigh 4kg or less, including the attachment system. …" ([6]).

A team of the ETH Zurich participates in the competition with a system, where a internal combustion engine and a generator supply electrical energy to the load [7]. The power electronic circuit to be analyzed consists of an AC-DC converter that rectifies the three-phase output of the generator, and a DC-DC buck-type converter that keeps the DC-output voltage at 28V (see **Fig.1**(a)). The inverter operates like a diode bridge to minimize the switching losses while the buck rectifier operates at a switching frequency of 250kHz to keep passive components small. Circuit parameters are given in **Tab.1**. A 48 hour-mission profile for the required output power (defined as "Profile A" in [8]) is shown in Fig.1(b).

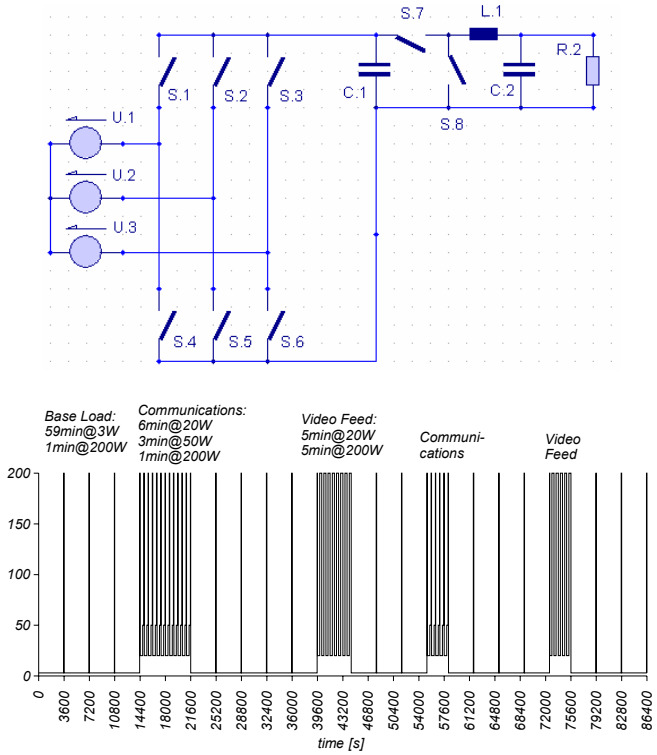


Figure 1. (a) Power circuit with inverter attached to a generator providing three-phase voltage. The DC-DC rectifier sets the output voltage to 28V. (b) "Load Profile A" for 48 hours [8]: 4x base load, 12x communications load, 5x base load, 8x video feed load, 3x base load, 5x communications load, 4x base load, 5x video feed load, 3x base load.

| | | | |
|---|---|---|---|
| $u_{PHASE,MAX}$ = = 18.2V | $C_1$ = 470uF | $C_2$ = 100uF (battery in prototype) | $L_1$ = 45uH |
| $f_{GENERATOR}$ = 330Hz | $f_{BUCK}$ = = 250kHz | MOSFET [9] @ 130°C: $k_{ON}$ = 2.38 uWs/W $k_{OFF}$ = 1.50 uWs/A $r_{ON}$ = 7.4mOhm | |

Table 1. Parameters of the power circuit Fig.1(a) and component properties.

In the following we will simulate the transient junction temperatures of all 8 semiconductors over the 48 hours load profile. In a second step we will evaluate the lifetime of the power electronic switches in comparison to a load profile with an equal energy requirement but reduced peak power.

## III. Transient Multi-Domain Simulation Circuit-Thermal

### A. General Simulation Strategy

The simulation strategy [10] for the coupled electric-thermal simulation is based on the following concepts:

- Employing a circuit simulator optimized for high-speed simulation of switched systems [4]
- Extracting a thermal impedance matrix from a 3D-structure of power module plus heat sink and convective cooling [11]
- Modeling transient switching losses of the power semiconductors employing a energy-pulse-counter scheme under consideration of the temperature-dependency of the losses [12]
- Maximizing the simulation speed of the thermal impedance matrix embedded in the circuit simulator via matrix splitting [13]

With the general strategy it is possible to realize full coupling of the physical domains.

This means that the switching losses are assumed to be temperature-dependent. In the example of the wearable power supply the DC-DC converter switching frequency is 250kHz which makes the numerical step width as small as $\Delta t$=20ns. Employing the simulator shown in Fig.2, performing a fully coupled simulation for the duration of one second took 37 minutes. Storing the data for 8 transient junction temperatures for one simulated second would require about 4.5GB on the hard disk. Most critical in the mission profile are the repeated 5 minutes of 200W during "video feed" followed by 5 minutes of 20W. Simulating these most critical 10 minutes would take 370 hours and/or 15 days. The theoretical amount of 2700GB simulation data would have to be significantly compressed. Typically, in such simulation tasks, it is not only simulation speed but also data handling which is critical.

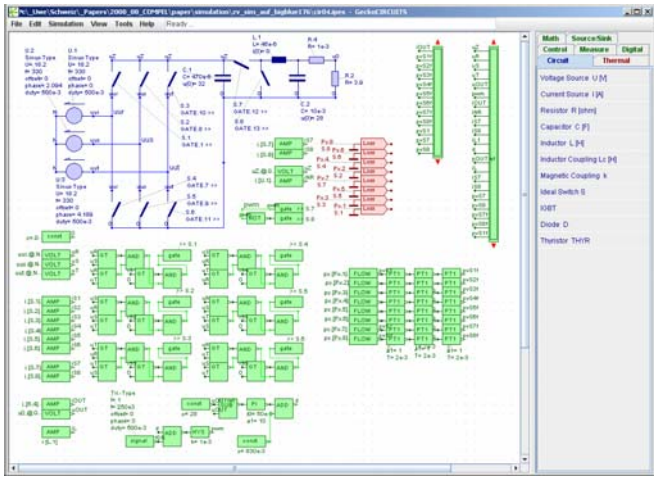

Figure 2. Power circuit (blue) and control circuit (green) for the wearable power supply. The transient losses of the semiconductors are delivered by the loss block (red) and are based on the loss parameters of the MOSFETs given in the datasheet (Tab.1). The employed multi-domain simulator GeckoCIRCUITS [4] has been developed at the PES/ETH Zurich.

*B. Applied Simulation Strategy and Results*

In order to perform the simulation with acceptable effort, the temperature-dependency of the semiconductor losses is neglected by assuming losses for 130°C. This gives a conservative design margin. The simulation is performed in five steps as listed below. If temperature-dependency of semiconductor losses should be considered, one has to go back with the results of (4) to step (2) as long as temperature errors occur.

(1) Simulate transient behavior of junction temperatures for step-change of load (e.g. 3W → 200W) to verify that the transient overshoot of the semiconductor losses (due to temporary current oscillations at load changes) does have negligible effect on the junction temperature time behavior.
(2) Simulate transient losses of all semiconductors for stationary operation of the converter system at a given output power (**Fig.2** and **Fig.3**). Do this for all output power levels as defined in the mission profile (3W, 20W, 50W, 200W, see **Tab.2**) under the assumption of $T_J$=130°C.
(3) Extract a compact thermal model from a detailed three-dimensional description of the MOSFETs on the PCB plus heat sink (**Fig.4** and **Fig.5**).
(4) Feed the compact thermal model with transient losses based on the defined load profile and the loss values calculated in (2) to get the junction temperatures of all 8 MOSFETs (**Fig.6** and **Fig.7**).

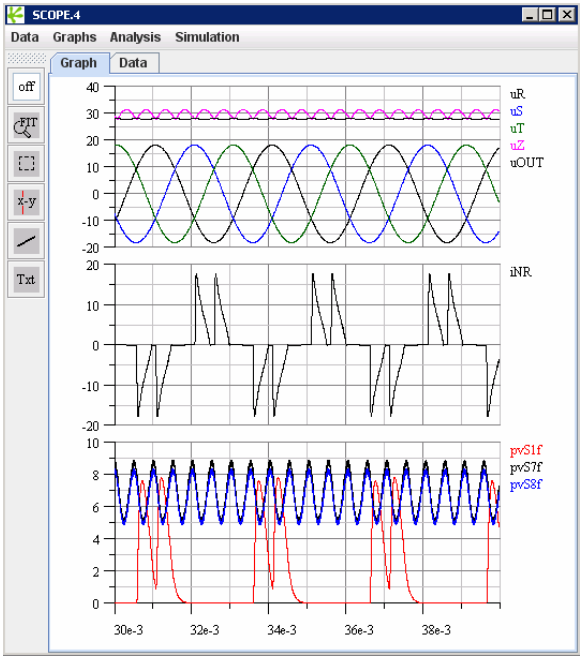


Figure 3. Simulated time-behavior of system properties for a stationary operation at 200W. (Top) The three-phase AC voltages uR, uS, uT, the inverter output voltage uZ and the buck output voltage uOUT; (Middle) the inverter AC side current of one phase iNR; (Bottom) first-order filtered transient semiconductor losses of the MOSFETs S1, S7 and S8.

Current oscillations at load changes typically occur in this application for durations of 0.2 seconds which means simulation times of around 8 minutes. Therefore, step (1) is not critical. For simulating the losses at stationary loads one just needs a few AC cycles resulting in simulation times below 5 minutes. Also step (2), resulting in the values of Tab.2, is not critical.

| | |
|---|---|
| $P_{OUT}$ = 3W / $R_{OUT}$ = 260ohm<br>$P_{V,S1,AVG}$ = 0.020W<br>$P_{V,S7,AVG}$ = 0.132W<br>$P_{V,S8,AVG}$ = 0.165W | $P_{OUT}$ = 20W / $R_{OUT}$ = 39ohm<br>$P_{V,S1,AVG}$ = 0.136W<br>$P_{V,S7,AVG}$ = 0.74W<br>$P_{V,S8,AVG}$ = 0.77W |
| $P_{OUT}$ = 50W / $R_{OUT}$ = 15.7ohm<br>$P_{V,S1,AVG}$ = 0.35W<br>$P_{V,S7,AVG}$ = 1.67W<br>$P_{V,S8,AVG}$ = 1.69W | $P_{OUT}$ = 200W / $R_{OUT}$ = 3.9ohm<br>$P_{V,S1,AVG}$ = 1.59W<br>$P_{V,S7,AVG}$ = 6.92W<br>$P_{V,S8,AVG}$ = 6.57W |

Table 2. Simulated average semiconductor losses at different stationary load conditions assuming $T_J$ = 130°C. Average losses are approximately equal for all six inverter MOSFETs S1, S2, S3, S4, S5 and S7.

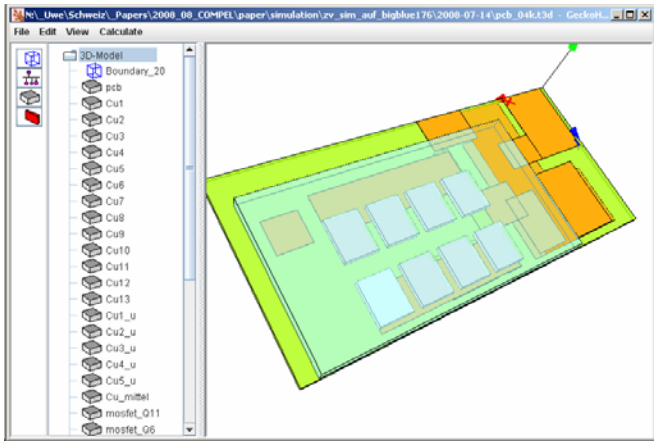


Figure 4. 3D-model of the 8 MOSFETs mounted onto a 4-layer PCB (green) with 35u-copper layers (orange). The aluminum plate (light blue) on top of the MOSFETs represents a small heat sink employing natural convection (1cm-fins every 4 mm → h = 30 W/Km$^2$). Natural convection (h = 15 W/Km$^2$) is assumed to be the dominating cooling mechanism on both sides of the PCB. The thermal 3D-simulator is part of GeckoCIRCUITS [4].

Setting up the 3D-model of the MOSFETs mounted onto the PCB including the heat sink plus the copper layer structures of the 4-layer PCB via schematic entry takes between 30minutes and 1 hour for the experienced user if a drawing of the PCB is already available.

Extracting a compact thermal model for the circuit simulator is time-consuming. The simulator shown in Fig.4 has a built-in algorithm that performs the extraction automatically ([11], [13]), but finding simulation parameters (e.g. acceptable error) of this procedure needs a couple of stationary and transient simulations which might take a couple of hours. The model extracting algorithm's effort is strongly model-dependent. In our application it takes between 15 and 20 hours and is typically done over night. In a next step it is planned to significantly increase the simulation speed of the thermal 3D-simulator by employing a Multigrid-Solver [14] instead of Gauss-Seidel [15] (as currently used).

The simulation of the transient junction temperatures shown in Fig.7 took about 9 minutes. As shown in Fig.7 the transient temperatures of all 8 switches show approximately equal temperatures because they are strongly thermally coupled by the heat sink.

The entire procedure to get the transient junction temperatures took about 24 hours calculation time with the main bottleneck of the extraction of the thermal model. With the implementation of the much faster Multigrid algorithm as a next step, we assume that this task will be done by about one order of magnitude faster [14]. The five-step approach also helped to keep control of the data size and the data accuracy because the data compression could be optimized for each individual step.

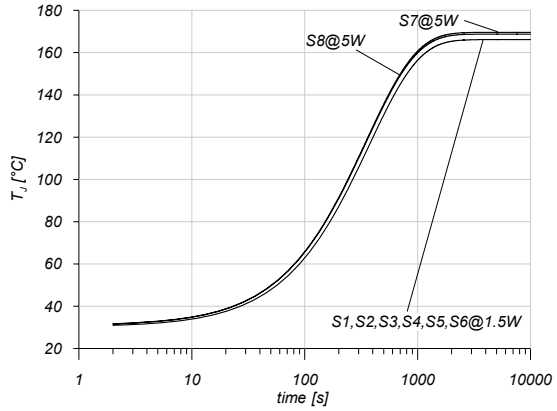


Figure 5. Transient thermal step responses of all 8 MOSFETs based on the thermal model shown in Fig.4. The curves are very close to each other due to the aluminum heat sink which provides strong thermal coupling.

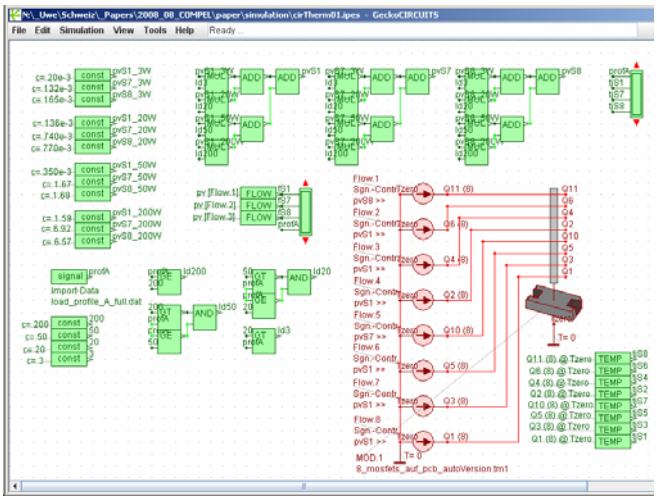

Figure 6. After loading the mission profile (Fig.1(b)) via a signal-block into GeckoCIRCUITS [4], the time behavior of the semiconductor losses based on the values of Tab.2 is defined employing the control blocks (green). The transient semiconductor losses are used to control the eight "power loss"-sources (red) that feed the transient losses into the symbol of the compact thermal model (extracted from the 3D-model shown in Fig.4). On the compact model's eight input terminals the according junction temperatures can be measured directly.

By applying the transient temperature to a physical stress-strain model in the next section, we will estimate the lifetime of the semiconductors of the power circuit. Because of lack of experimental data (accelerated testing via power cycling of the employed semiconductor [16]) we cannot give absolute lifetime estimates like "the semiconductors will survive X times Load Profile A". But we can give a relative lifetime comparison with a different mission profile. For demonstration of the proposed procedure we define in the following a modified load profile with its total energy consumption and duration unchanged (see **Fig.8**(a)). We call this new profile "*Load Profile M*". The corresponding junction temperature for Load Profile M is shown in Fig.8(b).

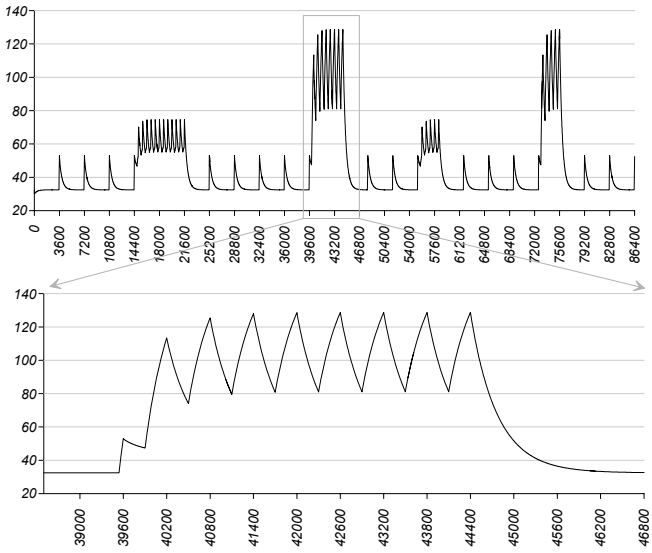

Figure 7. (a) Transient junction temperature [°C] of power semiconductor S7 simulated as shown in Fig.6 for Load Profile A (Fig.1(b)) over 48 hours [time-axis: 1hour/label ]; (b) Zoom into the most critical "Video Feed" mode [time-axis: 10min/label ].

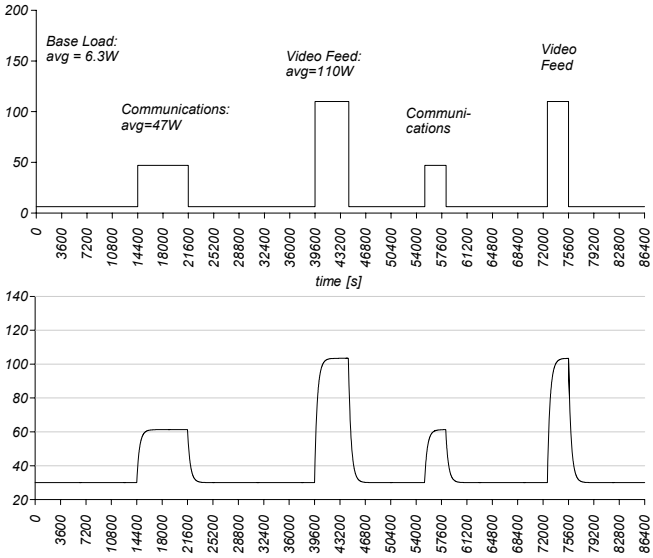


Figure 8. (a) Load Profile M defined for lifetime comparison. Energy content is equal to Load Profile A as shown in Fig.1(b). (b) Junction temperature time behavior [°C] for one semiconductor when Load Profile M is applied. See Fig.7(a) for a direct comparison.

## IV. Physical Modeling for Lifetime Estimation in Power Electronics

### A. *Physical Model of Metal-Interfaces Inside Power-Modules for Lifetime Estimation*

For our physical model, we basically follow the approach given in [17]-[24] with some modifications [25]. The first two equations of the stress-strain hysteresis model are given as

$$\gamma_{12}-\gamma_1=\frac{\tau_{12}-\tau_1}{G(T_1)}-C_P\cdot m\cdot|\tau_1|^{m-1}\frac{(\tau_{12}-\tau_1)}{G^m}\left(\frac{1+\mathrm{sgn}(\tau_1\cdot d\gamma)}{2}\right)$$

$$\gamma_{12}=-\frac{\tau_{12}}{K}+D_1(T_2-T_0) \tag{1}$$

with

$$G(T)=G_0+G_1\cdot T \tag{2}$$

and $G_0$ = 24782MPa, $G_1$ = 39.63MPa as defined for 63Sn37Pb [23]. A detailed parameter description of (1) is given in [17] and/or [24]. Furthermore, we define

$C_P$ … plastic strain coefficient
m … stress sensitivity of plastic strain

The stress reduction line employs two parameters K and $D_1$. K is dependent on the geometry of the solder connection and the layer-internal spring force, and $D_1$ is dependent on geometry of the solder interface and the mismatch of the heat expansion coefficient at the interface. Both parameters K and $D_1$ must be identified by fitting of experimental data.

Equation (1) describes elastic strain plus initial plastic strain. The second set of equations is given as

$$\gamma_2+\tfrac{1}{K}\tau_2=D_1(T_2-T_0)$$
$$\gamma_2-\gamma_{12}=\dot{\gamma}_{SS}(T_2,\tau_{12})\cdot\Delta t \tag{3}$$

with the secondary creep rate generally given as

$$\dot{\gamma}_{SS}=\dot{\gamma}_{SS1}+\dot{\gamma}_{SS2} \tag{4}$$

Depending on the stress level we employ Dislocation Control Creep or Diffusion Control Creep ([24]). In case of Dislocation Control Creep we have low-temperature dislocation glide process controlled creep

$$\dot{\gamma}_{SS1}=C_l\frac{G_2}{T_2+273}\cdot sign(\tau_{12})\cdot\sinh\left(\frac{\alpha|\tau_{12}|}{G_2}\right)^{n_l}e^{-\frac{Q_l}{8.62\cdot10^{-5}(273+T_2)}} \tag{5}$$

and high-temperature dislocation climb process controlled creep

$$\dot{\gamma}_{SS2}=C_h\frac{G_2}{T_2+273}\cdot sign(\tau_{12})\cdot\sinh\left(\frac{\alpha|\tau_{12}|}{G_2}\right)^{n_h}e^{-\frac{Q_h}{8.62\cdot10^{-5}(273+T_2)}} \tag{6}$$

where $C_l$ and $C_k$ are constants, $\alpha$ is a parameter related to power-law break down, and $n_l$ and $n_h$ are the stress exponents. Dislocation Control Creep can not accurately predict creep deformation at very low stresses. At the sufficiently low stress level, the creep process is controlled by diffusion [24]. Here, for Diffusion Control Creep the Coble creep model describes low-temperature grain boundary diffusional creep

$$\dot{\gamma}_{SS1}=B_1\frac{G_2}{T_2+273}\cdot\left(\frac{\tau_{12}}{G_2}\right)\cdot exp\left[-\frac{Q_B}{8.62\cdot10^{-5}(273+T_2)}\right] \tag{7}$$

and the Nabaro-Herring creep model describes high-temperature matrix diffusional creep

$$\dot{\gamma}_{SS2}=B_2\frac{G_2}{T_2+273}\cdot\left(\frac{\tau_{12}}{G_2}\right)\cdot exp\left[-\frac{Q_M}{8.62\cdot10^{-5}(273+T_2)}\right] \tag{8}$$

$B_1$ and $B_2$ are constants, $Q_b$ is the activation energy for grain boundary process, and $Q_M$ is the activation energy for matrix diffusional process. Equations (5) - (8) are valid dependent on the actual location in the temperature – stress plane as defined in [24]. After evaluation of the temperature – stress location at each simulation step, the relevant equation has to be selected.

### *B. Numerical Simulation of the Stress-Strain Characteristic*

With the parameters $C_l = 2\cdot10^{-5}$, $C_h = 0.25$, $Q_l = 48.5$, $Q_h = 81.5$, $\alpha = 1289$, $B_1 = 1.09\cdot10^{-17}$, $B_2 = 2.06\cdot10^{-8}$, $Q_b = 54.5$, $Q_m = 87.5$, $n_l = 5$, $n_h = 3$ taken from database and/or the literature [17] - [24], there remains a total of four parameters (K, $D_1$, m, $C_P$) to be found to correctly parameterize the physical model introduced in the previous section.

The procedure of parameterization starts with the assumption that we can apply the Norris-Landzberg [26] equation

$$\frac{N_{f,A}}{N_{f,B}}=\left(\frac{\Delta T_A}{\Delta T_B}\right)^{k1}\left(\frac{f_A}{f_B}\right)^{-k2}\cdot exp\left(\tfrac{E_a}{k}\cdot(T_{\max,B}^{-1}-T_{\max,A}^{-1})\right) \tag{9}$$

which takes into account not only temperature cycle (Coffin-Manson [27]) and absolute temperature (Arrhenius Law) but also the frequency of the cycling test.

With the thermal model of the MOSFET [9] one can perform numerical temperature simulations of various different cycling tests as shown in **Fig.9**. If a certain parameter set (K, $D_1$, m, $C_P$) is assumed, the physical model will give a hysteresis loop for each parameter test in the stress-strain plain as shown in **Fig.10**. If two different cycling tests of Fig.9 give a certain ratio of the number of cycles to failure $r_f = N_{f,A}/N_{f,B}$ according to the Norris-Landzberg equation (9), then the ratio of the hysteresis areas (Fig.10) of these two cycling tests must give the same ratio. This is because the area of the hysteresis loop represents the energy damage per cycle. If the accumulated energy damage reaches a certain level the device will fail.

This must be valid for all possible combinations of cycling tests. If the parameter set (K, $D_1$, m, $C_P$) is chosen correctly by a search algorithm applied to this parameterization problem, the condition is fulfilled.

Fig.10 shows the hysteresis loops for a set (K, $D_1$, m, $C_P$) where the maximum error is 1.67 (deviation of 67% from ideal matching). Since cycling test results often stray by a factor 2 or more (see [28] for an excellent overview), we assume this to be an acceptable solution. The search algorithm applied needed about 15 minutes calculation time to find this optimum parameter set.

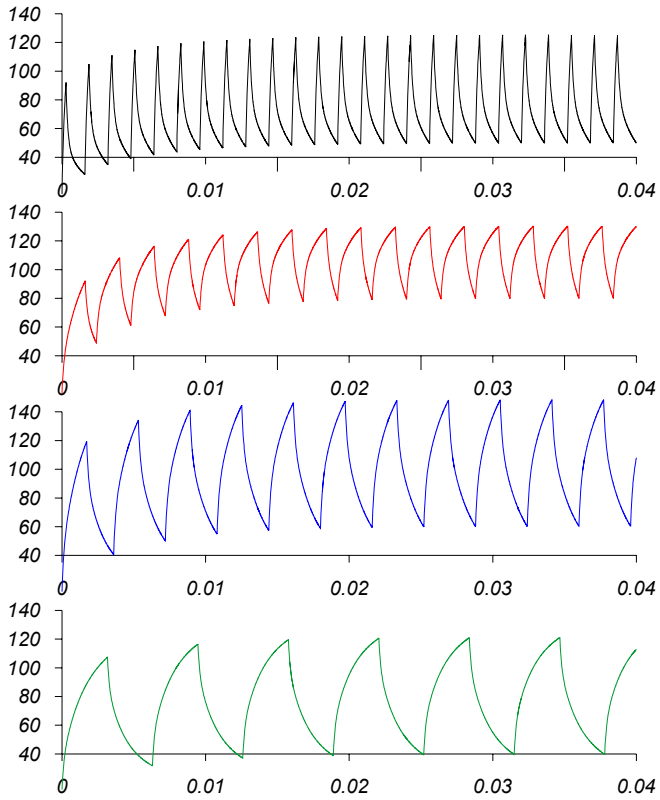


Figure 9. Simulation of the time-behaviour of the junction temperatures [°C] of four cycling tests based on the thermal model of the MOSFET [9]. **(a)** Pv=320W / f=625Hz / $d_{ON}$=0.1768; **(b)** Pv=137W / f=417Hz / $d_{ON}$=0.6749; **(c)** Pv=179W / f=278Hz / $d_{ON}$=0.4788; **(d)** Pv=127W / f=159Hz / $d_{ON}$=0.5036.

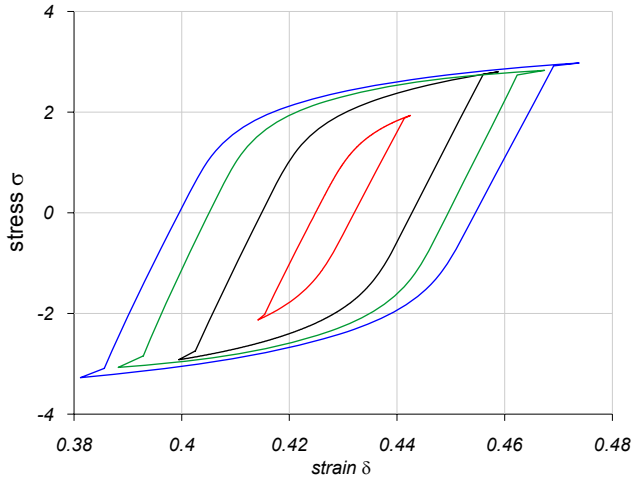


Figure 10. Simulation of a single hysteresis loop in the stress-strain plane for the four cycling tests described in Fig.9. The parameters of the underlying physical model found by the search algorithm are (K=2000, $D_1$=4.59·10$^{-5}$, m=4.4, $C_P$=28.3·10$^{-12}$). This parameter set results in a parameterization error of 1.67.

If the number of cycles to failure $N_f$ is known for at least one experiment, the physical model is able to estimate the lifetime for a certain mission profile in absolute terms: If one knows the damage energy per cycle (hysteresis area), and one knows the number of cycles to failure, then the total damage energy for the device can be calculated directly. If, for an arbitrary mission profile, the strain is integrated over the stress based on the physical model, the accumulated damage energy for that mission profile is found. If the total damage energy for the device is divided through the accumulated damage energy for the mission profile, one gets the number of missions to failure.

In our investigation we do not have experimental cycling test data for the employed MOSFET [9]. Therefore, we can only perform a relative comparison between different mission profiles. In order to find the impact on lifetime for two different mission profiles (*Load Profile A*, Fig.1(a), vs. *Load Profile M*, see definition at the end of the previous section) we will apply in the following the according temperature profiles to our physical model.

## V. Numerical Simulation of Long-Term Mission Profiles

Integrating stress along strain gives a value proportional to deformation energy. Stress and strain are not clearly defined in this model, so the integration gives a value that can only be used to compare different mission profiles or has to be parameterized by at least one cycling experiment (see previous section). In Fig.11 the stress-strain curves for *Load Profile A* and *Load Profile M* are shown in a three-dimensional representation. Integration and division gives the ratio

$$r_I = \int_{Profile\,A} \sigma(\delta)\, d\delta \Big/ \int_{Profile\,M} \sigma(\delta)\, d\delta = 7.8 \qquad (10)$$

which means that *Profile A* results in 7.8 times more deformation damage than *Profile M*. Therefore, applying *Profile M* will result in an increase of the lifetime of the semiconductors by a factor 7.8 as compared to the application of *Profile A*. This means that 7.8 more missions of Type M can be performed than of Type A. If data of an experimental cycling test would be available it would be possible to make absolute lifetime estimations for both load profiles.

The numerical simulations shown in Fig.11 took more than 2 days calculation time for each one. This is due to the simulation time step that has to be set to a very small value (by about a factor 100 smaller than for the temperature simulations shown in Fig.7 and Fig.8(b)) in order to achieve numerical stability of the physical model (1) – (8). Still one can clearly see small numerical oscillations of the curves shown in Fig.11. The result of a relative lifetime difference of a factor 7.8 (see equation (10)) needs experimental verification which is part of a research project currently performed at the PES / ETH Zurich. For verification it is also necessary to analyze the numerical stability of the physical model in much greater detail, to speed up the numerical procedures, and to study the sensitivity of the physical model concerning parameter changes. This research is currently performed [25] and will show if the proposed procedure is reliable enough to be introduced in the power electronics design process.

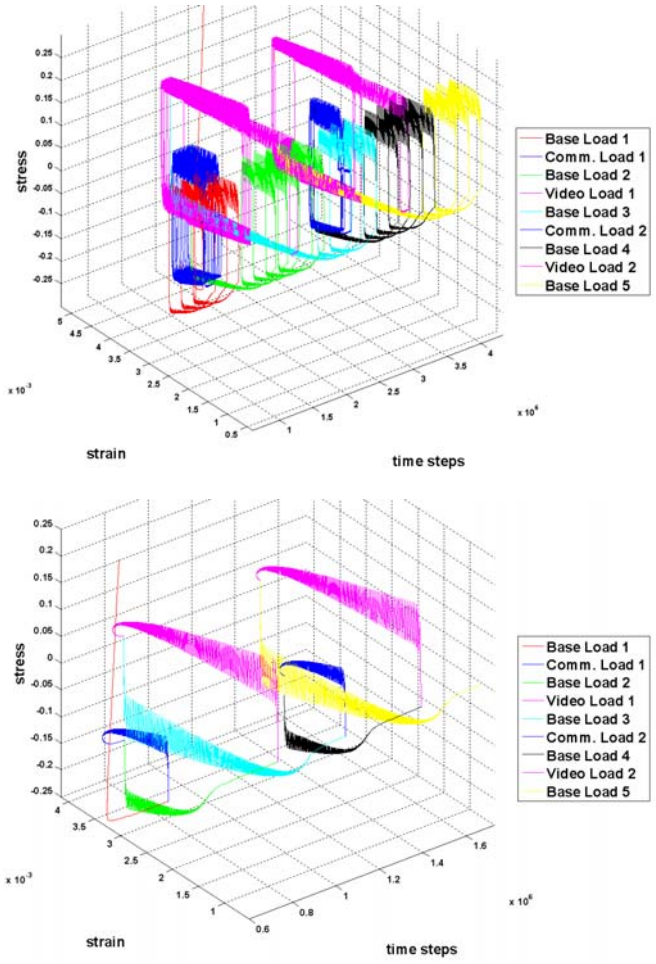


Figure 11. Simulation of the time-dependent stress-strain relation for (a) *Load Profile A* and (b) *Load Profile M*. Parameters of the physical model are set according to the previous section and caption of Fig.10.

## VI. Summary

We demonstrated the numerical calculation of the semiconductor lifetime of the power electronics of a wearable power supply (96 hours operation at 3W with short peaks of 20W, 50W and 200W, and a weight of 4kg). With a total simulation effort of about 4 days it was possible to calculate the relative lifetime ratio for two different mission profiles. The physical lifetime model proposed is very promising but needs more detailed theoretical analysis and experimental verification before it can be applied in the power electronics design procedure.

## References


[1] E. Wolfgang, "Mission Profiles", *ECPE-Sem. Zuverlässigkeit leistungselektr. Systeme*, Nuremberg, Germany, Oct. 17 - 18, 2007

[2] M. Ciappa, F. Carhognani, P. Cow, W. Fichtner, "Lifetime Prediction and Design of Reliability Tests for High-Power Devices in Automotive Applications", *IEEE Trans. on Device and Materials Reliability*, Vol.3, No. 4, Dec. 2003

[3] M. Ciappa, "Lifetime prediction on the Base of Mission Profile", *Microelectronics Reliability* 45 1293-1298, 2005

[4] Gecko-Research at www.gecko-research.com

[5] Wearable Power Prize 2008 competition of the US Department of Defense, overview published at http://www.dod.mil/ddre/prize/topic.html

[6] Wearable Power Prize 2008 competition: Rules published at http://www.dod.mil/ddre/prize/doc/Wearable_Power_RulesV6_1.pdf

[7] I. Kovacevic, S. D. Round, J. W. Kolar, K. Boulouchos, "Optimization of a Wearable Power System", *Proc. of the 11th IEEE Workshop on Control and Modeling for Power Electronics (COMPEL 2008),* Zurich, Switzerland, Aug. 18 – 20

[8] Wearable Power Prize 2008 competition: Load Profiles for 48 Hours of the 92 Hours Bench Test published at http://www.dod.mil/ddre/prize/doc/Load_Profile_Bench_Test.pdf

[9] IRLR3114ZPbF from International Rectifier, datasheet published at http://www.irf.com/product-info/datasheets/data/irlr3114zpbf.pdf

[10] U. Drofenik, D. Cottet, A. Müsing, J. W. Kolar, „Design Tools for Power Electronics: Trends and Innovations", *Ingenieurs de l'automobile*, No. 791, pp. 55 – 62, Dec. 2007

[11] U. Drofenik, D. Cottet, A. Müsing, J.-M. Meyer, J. W. Kolar, "Modelling the Thermal Coupling between Internal Power Semiconductor Dies of a Water-Cooled 3300V/1200A HiPak IGBT Module", *Proc. of the Conf. for Power Electronics, Intelligent Motion, Power Quality (PCIM'07)*, Nuremberg, Germany, May 22 - 24, 2007

[12] U. Drofenik, J. W. Kolar, "A General Scheme for Calculating Switching- and Conduction-Losses of Power Semiconductors in Numerical Circuit Simulations of Power Electronic Systems", *Proc. of the 2005 International Power Electronics Conference (IPEC'05)*, Niigata, Japan, April 4 - 8, CD-ROM, ISBN: 4-88686-065-6, 2005

[13] U. Drofenik, D. Cottet, A. Müsing, J.-M. Meyer, J. W. Kolar, "Computationally Efficient Integration of Complex Thermal Multi-Chip Power Module Models into Circuit Simulators", *Proceedings of the 4th Power Conversion Conference (PCC'07)*, Nagoya, Japan, April 2 - 5, CD-ROM, ISBN: 1-4244-0844-X, 2007

[14] S. V. Patankar, "Numerical Heat Transfer and Fluid Flow", ISBN 0-89116-522-3, Taylor & Francis, 1980.

[15] W. H. Press, S. A. Teukolsky, W. T. Vetterling, B. P. Flannery, "Numerical Recipes in C: The Art of Scientific Computing", 2nd edition, ISBN 0-521-43108-5, Cambridge University Press, 1992.

[16] W. G. Ireson, C. F. Coombs Jr., R. Y. Moss, "Handbook of Reliability Engineering and Management", 2nd edition, ISBN 0-07-012750-6, McGraw-Hill, 1995.

[17] J.-P. Clech, "Review and Analysis of Lead-Free Solder Material Properties", published at http://www.metallurgy.nist.gov/solder/

[18] J-P. Clech, "Solder Reliability Solutions: a PC-based design-for-reliability tool", *Proceedings, Surface Mount International Conference*, Sept. 8-12, 1996, San Jose, CA, Vol. I, pp. 136-151. Also in *Soldering and Surface Mount Technology, Wela Publications, British Isles*, Vol. 9, No. 2, pp. 45-54, July 1997

[19] P. Lall et al., "Decision-support models for thermo-mechanical reliability of lead-free flip-chip electronics in extreme environments," in *Proc.s 55th Electronics Components Technology Conference*, Orlando, FL, pp. 127–136, May/Jun. 31–3, 2005

[20] S. Knecht, L. R. Fox, "Constitutive Relation and Creep-Fatigue Life Model for Eutectic Tin-Lead Solder", *IEEE Trans. on Components, Hybrids, and Manufacturing Technology*, Vol. 13, No. 2, June 1990

[21] S. Knecht, L. Fox, "Integrated matrix creep: application to accelerated testing and lifetime prediction", *Chapter 16, Solder Joint Reliability: Theory and Applications*, ed. J. H. Lau, Van Nostrand Reinhold, pp. 508 - 544, 1991

[22] D. Rubesa, "Lifetime Prediction and Constitutive Modeling for Creep-Fatigue Interaction", ISBN 3-443-23015-6, Berlin, Germany: Borntraeger, 1991

[23] X.Q. Shi, Z.P. Wang, Q.J. Yang, H.L.J. Pang, Creep Behavior and Deformation Mechanism Map of SnPb Eutectic Solder Alloy, *Journal of Engineering Materials and Technology*, Jan 2003, Vol. 125

[24] G. Z. Wang, Z. N. Cheng, K. Becker, J. Wilde, Applying ANAND Model to Represent the Viscoplastic Deformation Behaviour of Solder Alloys, *Journal of Electronic Packaging* , Sept. 2001,Vol. 123, Issue 3, pp. 247-253

[25] I. Kovacevic, "Physical Models for Lifetime Estimation in Power Electronics", Master thesis at the PES / ETH Zurich, 2008.

[26] K. C. Norris, A. H. Landzberg, "Reliability of controlled collapse interconnections," *IBM J. Res. Dev.*, vol. 13, no. 3, pp. 266–271, May 1969.

[27] S. S. Manson, Thermal Stress and Low Cycle Fatigue. New York: McGraw-Hill, 1966.

[28] R. Bayerer, T. Herrmann, T. Licht, J. Lutz, M. Feller, "Model for Power Cycling Lifetime of IGBT Modules – Various Factors Influencing Lifetime", *Proc. of the 5th International Conf. on Integrated Power Electronics Systems (CIPS'08)*, Nuremberg, Germany, March 11 - 13, 2008.